

Molecular and Biological Characterization of Human Monoclonal Antibodies Binding to the Spike and Nucleocapsid Proteins of Severe Acute Respiratory Syndrome Coronavirus

Edward N. van den Brink,¹ Jan ter Meulen,¹ Freek Cox,¹ Mandy A. C. Jongeneelen,¹
Alexandra Thijsse,¹ Mark Throsby,¹ Wilfred E. Marissen,¹ Pauline M. L. Rood,¹
Alexander B. H. Bakker,¹ Hans R. Gelderblom,² Byron E. Martina,³
Albert D. M. E. Osterhaus,³ Wolfgang Preiser,⁴
Hans Wilhelm Doerr,⁴ John de Kruif,¹
and Jaap Goudsmit^{1*}

Cruell Holland B.V., Leiden,¹ and Institute of Virology, Erasmus Medical Center, Rotterdam,³ The Netherlands, and Robert Koch Institute, Berlin,² and Institute for Medical Virology, Johann Wolfgang Goethe University, Frankfurt am Main,⁴ Germany

Received 12 July 2004/Accepted 8 September 2004

Human monoclonal antibodies (MAbs) were selected from semisynthetic antibody phage display libraries by using whole irradiated severe acute respiratory syndrome (SARS) coronavirus (CoV) virions as target. We identified eight human MAbs binding to virus and infected cells, six of which could be mapped to two SARS-CoV structural proteins: the nucleocapsid (N) and spike (S) proteins. Two MAbs reacted with N protein. One of the N protein MAbs recognized a linear epitope conserved between all published human and animal SARS-CoV isolates, and the other bound to a nonlinear N epitope. These two N MAbs did not compete for binding to SARS-CoV. Four MAbs reacted with the S glycoprotein, and three of these MAbs neutralized SARS-CoV in vitro. All three neutralizing anti-S MAbs bound a recombinant S1 fragment comprising residues 318 to 510, a region previously identified as the SARS-CoV S receptor binding domain; the nonneutralizing MAb did not. Two strongly neutralizing anti-S1 MAbs blocked the binding of a recombinant S fragment (residues 1 to 565) to SARS-CoV-susceptible Vero cells completely, whereas a poorly neutralizing S1 MAb blocked binding only partially. The MAb ability to block S1-receptor binding and the level of neutralization of the two strongly neutralizing S1 MAbs correlated with the binding affinity to the S1 domain. Finally, epitope mapping, using recombinant S fragments (residues 318 to 510) containing naturally occurring mutations, revealed the importance of residue N479 for the binding of the most potent neutralizing MAb, CR3014. The complete set of SARS-CoV MAbs described here may be useful for diagnosis, chemoprophylaxis, and therapy of SARS-CoV infection and disease.

Severe acute respiratory syndrome (SARS) was first identified in 2002 as a newly emerging disease in Guangdong Province, China. The disease, associated with unusual atypical pneumonia, spread in 2003 to over 30 countries worldwide with more than 8,000 reported cases and an estimated 55% mortality among the elderly (9). A virus was isolated from tissues of SARS patients (10, 21, 23, 32) and a SARS-associated coronavirus (SARS-CoV), a new member in the family of *Coronaviridae*, was identified as the causative agent fulfilling Koch's postulates (12).

The clinical course of SARS is highly variable (31) after a relatively short 6- to 10-day incubation period (9). In ca. 20% of the patients, SARS-CoV infection progresses to a stage of respiratory failure requiring ventilation support. Overall, 10% of the patients, ca. 6.8% of patients younger and 55% of patients older than 60 years of age (9), die as a consequence of immunopathological lung damage caused by a hyperactive antiviral immune response (29).

Antibodies to SARS-CoV become detectable in patient's

serum between days 10 and 15 and correlate with a decline in viral loads. More than 93% of the patients were reported to have seroconverted by day 28 (31). The pattern of SARS-CoV replication and development of a neutralizing immune response observed in experimentally infected mice largely resembles the course of infection in SARS patients. Passive transfer of polyclonal immune serum has been shown to reduce pulmonary virus titers in this mouse model of SARS-CoV infection (37). Therefore, immunoprophylaxis of SARS-CoV infection with antibodies might be a viable SARS control strategy.

The S1 domain of other previously characterized CoV S proteins harbors the binding sites for CoV neutralizing antibodies (3, 4, 13, 22). Shortly after identification of angiotensin-converting enzyme 2 (ACE2) as a natural receptor for SARS-CoV infectivity (25), the putative ACE2 receptor-binding site was first narrowed down to a region between residues 303 to 537 (43) and later to residues 318 to 510 (42) within the S1 domain (residues 1 to 672) of the S protein (42). Sui et al. selected the first human monoclonal antibodies (MAbs) to the SARS-CoV S protein by antibody phage display by using a fragment corresponding to the S1 domain (38). One of these S1 MAbs was capable of neutralizing SARS-CoV infectivity by blocking the association with ACE2 (38). Recent evidence

* Corresponding author. Mailing address: Cruell Holland B.V., P.O. Box 2048, 2301 CA Leiden, The Netherlands. Phone: 31-71-5248701. Fax: 31-71-5248702. E-mail: j.goudsmit@cruell.com.

TABLE 1. List of mutations introduced in recombinant S fragment S318-510 (residues 318 to 510) of the FM1 sequence^a

Mutant	Mutation(s)	Strain	GenBank no.
S318-510 (FM1)		FM1	AY291315
Mutant 1	K344R	GZ02	AY390556
Mutant 2	S353F	Sin3408	AY559083
Mutant 3	R426G, N437D	Shanghai LY	AY322207
Mutant 4	Y436H	GZ-C	AY394979
Mutant 5	Y442S	Sino1-11	AY485277
Mutant 6	N479S	BJ302 cl.2	AY429073
Mutant 7	K344R, F360S, L472P, D480G, T487S	GD03T0013	AY525636
Mutant 8	K344R, F501Y	GD01	AY278489

^a The amino acid substitutions in the S region (residues 318 to 510) compared to the FM1 and GenBank accession numbers of the corresponding SARS-CoV strain or S gene are indicated.

suggested the presence of antigenic determinants in the S1 (46), as well as in the S2 domain of the S protein (44). We set out to isolate MABs by antibody phage display selections by using whole SARS-CoV virions, which not only allows for the selection selected of neutralizing MABs against S but also for MABs against other structural viral proteins. The SARS-CoV neutralizing capacity of one of the isolated MABs, CR3014 was recently established (39). We demonstrated that CR3014 reduced replication of SARS-CoV in the lungs of infected ferrets, abolished shedding of SARS-CoV in pharyngeal secretions, and completely prevented the development of virus-induced macroscopic lung pathology.

In the present study, we characterized human MAB CR3014 and the other MABs that were selected against SARS-CoV virions in more detail. We mapped the MAB binding sites within the structural proteins N and S and identified the in vitro neutralizing mechanism of CR3014 responsible for the observed reduced viral replication in vivo.

MATERIALS AND METHODS

Virus preparation. Gamma-irradiated SARS-CoV (Frankfurt 1 strain FM1) (7, 35) used for panning was prepared as follows. Medium from SARS-CoV-infected Vero cells was harvested 3 days postinfection and cleared by centrifugation to remove cell debris. The cleared supernatant was applied on a 25% glycerol cushion, and SARS-CoV was pelleted by centrifugation for 2 h at 25,000 rpm at 4°C in a Beckman SW28 rotor. SARS-CoV was resuspended in 10 mM Tris-HCl (pH 7.4)–1 mM EDTA–200 mM NaCl and gamma-irradiated with 45 kGy on dry ice to abolish infectivity.

Selection of SARS-CoV-binding clones by phage panning. Single-chain variable antibody fragments (scFv) were selected by using antibody phage display libraries and technology, essentially as described previously (8). Maxisorp Immunotubes (Nunc, Roskilde, Denmark) were coated overnight at 4°C with gamma-irradiated SARS-CoV virions. To eliminate nonspecific binding, the phage library was first adsorbed in phosphate-buffered saline (PBS) containing 10% fetal bovine serum (FBS) and 2% nonfat dry milk. Subsequently, phages were incubated with SARS-CoV in the presence of 0.05% Tween 20 for 2 h at room temperature or at 37°C. Unbound phages were removed by 10 washes with PBS containing 0.05% Tween 20, followed by 10 washes with PBS. Bound phages were eluted and used to reinfect *Escherichia coli* XL1-Blue (Stratagene, La Jolla, Calif.) and reamplified as described previously (27). After each round of selection, phages from individual colonies were tested for binding to SARS-CoV and FBS as a negative control antigen in an enzyme-linked immunosorbent assay (ELISA).

Human IgG antibody production and purification. The engineering and production of the human immunoglobulin G1 (IgG1) MABs was essentially performed as described previously (2). The variable regions of scFv were recloned into separate vectors for IgG1 heavy- and light-chain expression. Variable heavy (VH)- and light (VL)-chain regions from each scFv were PCR amplified by using specific primers to append restriction sites and restore complete human frameworks. IgG1 MABs were expressed as described previously (2). Subsequently, the

harvested supernatants were purified on protein A columns, followed by buffer exchange in PBS over size exclusion columns.

Immunofluorescence. Reactivity with SARS-CoV-infected cells by the human IgG1 MABs was assessed by indirect immunofluorescence according to the manufacturer's instructions (Euroimmun AG, Lubeck, Germany).

Expression of N and soluble truncated S glycoproteins. DNA encoding for the N protein was amplified from total random hexamer cDNA prepared from the SARS-CoV FM1 isolate by using the oligonucleotide primers KpnINCFOR 5'-C TTGGTACCGCCACCATGTCTGATAATGGACC-3' and XbaINCFOR 5'-GT TCTCTAGATGCCTGAGTTGAATCAGC-3' and cloned as a KpnI-XbaI fragment in pAdapt/myc-HisA, a modified pAdapt vector that adds a C-terminal myc and His tag to the protein. The cDNA encoding the complete FM1 S protein was optimized for optimal expression by Geneart (Regensburg, Germany), followed by cloning in the pAdapt vector (17). DNA encoding for the N-terminal 565 amino acids of the S protein (S565) was cloned as a KpnI-BamHI fragment in pAdapt/myc-HisC. A fragment corresponding to residues 318 to 510 of S was amplified on S gene cDNA by using the oligonucleotide primers EcoRIspike-For318 (5'-CCTGGAATTCTCCATGGCCAACATCACCAACC-3') and XbaIspikeRev510 (5'-GAAGGGCCCTCTAGACACGGTGGCAGG-3'). The resulting fragment was digested with EcoRI-XbaI and cloned into pHAVT20/myc-HisA to yield pHAVT20/myc-HisA S318-510. In this vector expression of fragment S318-510 fused to the HAVT20 leader sequence was under control of the human, full-length, immediate-early cytomegalovirus promoter. S and N constructs were transfected in human 293T cells for transient protein expression. Soluble N protein was recovered by lysis of the transfected cells in 150 mM NaCl–1% NP-40–0.1% sodium-dodecyl sulfate (SDS)–0.5% deoxycholate–50 mM Tris (pH 8), whereas fragments S565 and S318-510 were purified from culture supernatant by using Ni-NTA (Qiagen, Hilden, Germany).

Construction of variant S318-510 fragments. To investigate whether anti-S MABs recognize the S protein of all currently known human SARS-CoV isolates, recombinant S fragments harboring the different amino acid substitutions as shown in Table 1 were generated. The amino acid substitutions were introduced in the pHAVT20/myc-HisA S318-510 vector by using the QuikChange II site-directed mutagenesis kit (Stratagene). Mutagenic oligonucleotide primers were designed according to the manufacturer's instructions. To exclude the introduction of additional mutations in the plasmid outside the gene of interest, the mutated (592-bp EcoRI-XbaI) fragment was recloned in EcoRI-XbaI-cut pHAVT20/myc-HisA. The resulting plasmids were transfected into 293T cells for transient protein expression as described above.

Target identification with ELISA. ELISAs with captured S and N fragments were performed as follows. Microtiter plates were coated overnight with 5 µg of anti-myc antibody (Roche Molecular Biochemicals, Mannheim, Germany)/ml in 50 mM bicarbonate buffer (pH 9.6). After being washed with PBS containing 0.05% Tween 20, the wells were blocked for 1 h in 1% nonfat dry milk, followed by incubation of the myc-tagged S and N fragments, followed by the addition of various concentrations of human IgG1 MABs or horseradish peroxidase (HRP)-conjugated anti-His6 (Roche) for 1 h each at room temperature. Bound human IgG was detected by HRP-conjugated mouse anti-human IgG (Jackson ImmunoResearch Laboratories) and further developed with O-phenylenediamine substrate (Sigma FAST OPD; Sigma). The reaction was stopped by the addition of 1 M H₂SO₄, and the absorbance was measured at 492 nm.

Competition ELISA. Using a setup similar to that described above, competition ELISAs were performed. Captured SARS-CoV or S565 fragment was incubated with nonsaturating amounts of biotinylated IgG in the presence or absence of competing IgG. Bound biotinylated IgG was detected with strepta-

vidin-conjugated HRP (BD Pharmingen, San Diego, Calif.) and developed as described above.

Epitope mapping. Two sets of 2,740 overlapping 15-mer linear and looped peptides were synthesized on the basis of all open reading frames encoded by the SARS-CoV Urbani viral genome except for the replicase protein (Pepscan Systems, Lelystad, The Netherlands). Peptides were coupled to a solid support, and epitope mapping of the IgGs was performed by using the Pepscan method described previously (14, 15, 34). The covalently linked peptides were incubated overnight at 4°C with 1 µg of IgG/ml in PBS containing 5% horse serum and 5% ovalbumin, and bound antibody was detected.

Electron microscopy. Immunoelectron microscopy (immuno-EM) of SARS-CoV-infected Vero cells was performed essentially as described previously (1). Bound MABs were detected by incubation with anti-hu-IgG-5-nm gold conjugates (British Biocell International, Cardiff, United Kingdom), and ultrathin sections were evaluated under a ZEISS EM 10A transmission electron microscope.

Flow cytometry analysis. Spike (S)-transfected 293T cells were incubated with human IgGs at a concentration of 10 µg/ml for 1 h on ice. Cells were washed three times and incubated for 45 min with biotinylated goat anti-human IgG, followed by a 10-min incubation with streptavidin-conjugated phycoerythrin (Caltag, South San Francisco, Calif.), and then analyzed on a FACSCalibur with CELLQuest Pro software (Becton Dickinson).

Vero cells expressing ACE2 were incubated for 1 h at 4°C with saturating concentrations of the S565 fragment in the presence or absence of 0.5 µM IgG. After three washes, bound S565 fragment was detected by using biotinylated anti-myc antibody (Santa Cruz Biotechnology, Inc., Santa Cruz, Calif.) and streptavidin-conjugated phycoerythrin. All incubations and washes were performed at 4°C in PBS supplemented with 0.5% bovine serum albumin.

Neutralization assay. SARS-CoV neutralizing activity of scFv and IgG1 MABs were titrated in an assay that measures neutralization of a known amount of virus. ScFv and IgGs were screened in serial twofold dilutions in Dulbecco modified Eagle medium containing 5% FBS. A 50-µl aliquot of the scFv and MAB dilutions was mixed with 50 µl of SARS-CoV containing 100 50% tissue culture infective doses (TCID₅₀) for scFv and 10, 30, or 100 TCID₅₀ for IgGs and then incubated for 1 h at 37°C. The antibody-SARS-CoV mixture was incubated in triplicate into 96-well plates containing an 80% confluent monolayer of Vero cells. The Vero cells were cultured for 5 days at 37°C and monitored for the development of cytopathic effects. The complete absence of cytopathic effect in an individual culture well was defined as protection.

Data deposition. Sequences are available from GenBank under accession numbers AY554173 to AY554183.

RESULTS

Selection and identification of MABs to SARS-CoV. To obtain human MABs to SARS-CoV, we screened scFv-phage libraries for binding to gamma-irradiated SARS-CoV virions coated on plastic. After two or three rounds of selection, testing of 1,138 individual colonies by ELISA resulted in 96 clones that specifically recognized SARS-CoV. Sequence analysis of these SARS-CoV binding colonies revealed the presence of eight unique clones (Fig. 1A). The selected scFv were encoded by eight different VH sequences and three different VL sequences (Fig. 2). The VH sequences were derived from several germ line genes of the VH3 family. The VL sequences of clones CR3006 and CR3015 were encoded by germ line genes A20 and V2-13 of the VκI and Vλ3 families, respectively. The third VL sequence, derived from the VκI O2 germ line gene, was identified in the remaining six clones (CR3001, CR3002, CR3009, CR3013, CR3014, and CR3018). The genes encoding the scFv were recloned and expressed as fully human IgG1 antibody molecules.

Specificity of MABs for SARS-CoV. First, we tested whether the fully human IgG1 molecules were capable of binding the antigen used for panning. As shown in Fig. 1B, all IgGs were able to bind gamma-irradiated SARS-CoV virions, but to different extents. To further confirm the specificity of our IgGs for the virus, immunofluorescence was performed on SARS-

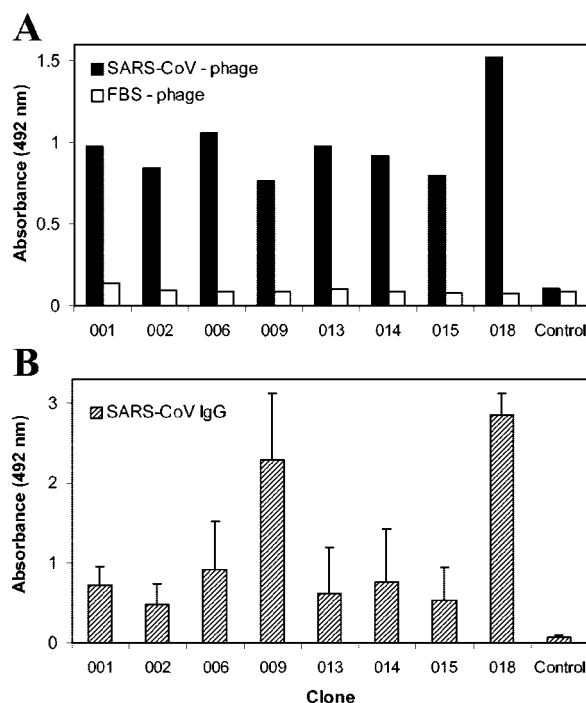


FIG. 1. Selective binding of isolated scFv phage antibodies to SARS-CoV by ELISA. (A) Phage produced from individual colonies were analyzed for binding to SARS-CoV or FBS coated on microtiter wells. (B) Binding of IgGs constructed from the isolated scFv to SARS-CoV.

CoV-infected (Fig. 3) and noninfected Vero cells (data not shown). All of the IgGs specifically stained SARS-CoV-infected Vero cells, whereas control IgG did not.

Characterization of antibodies binding N. A preliminary radioimmunoprecipitation assay performed to identify the SARS-CoV proteins recognized by the isolated MABs yielded proteins migrating at a molecular weight of 46,000 or 180,000, which most likely represent nucleocapsid (N) or S protein (data not shown). To confirm the antigen recognized by the panel of anti-SARS IgGs, the interaction with N protein, the most abundant viral protein, was evaluated by ELISA. N protein recovered from transfected 293T cells was captured on an ELISA plate, followed by incubation with the anti-SARS IgGs. Figure 4A shows that IgG CR3009 and CR3018 bound specifically to N protein. In order to rank the affinities of the MABs, a titration of the IgG concentration was performed. Titration of the MABs showed that CR3009 bound slightly better to N protein than did CR3018 (Fig. 4B), which may reflect a difference in affinity. To further explore the antibody binding sites within the N protein, a competition ELISA on immobilized SARS-CoV was performed (Fig. 4C). The results show that binding of biotinylated IgG CR3009 and CR3018 is not or hardly affected in the presence of excess of unlabeled IgG CR3018 and CR3009, respectively. As expected binding of the biotinylated anti-N MABs is blocked by their unlabeled counterparts but not by anti-S MAB CR3014. This demonstrates that IgG CR3009 and CR3018 do not compete with each other for binding to N protein and most likely recognize different epitopes.

VH

	FR1	CDR1	FR2	CDR2	FR3	CDR3	FR4	
	EVQLVESGGGLVQP	GGSLRLS	CAASGFTFS	DYSMS	NVRQAPGKGL	EWVS	RISGKNGSGSTYY	ADSVKGRPTISRDN
	SK	GL	Y	Q	Y	AD	SV	K
CR3001K.....	G..NGSRTN
CR3002K.....	G..NG	TRN.A.YT.E.A.DKT	3-38
CR3006K.....	G.P.HA	V.YD--SNKTK	DG--PS	3-72
CR3009V.....R.....P.NSSTK	FMVT.Y	3-30
CR3013V.....R.....P.NSSTK	FMVT.Y	3-23
CR3013V.....R.....P.NS	TRN.A.YT.E.A.DKTK	3-72
CR3014V.....R.....P.NS	TRN.A.YT.E.A.DKTK	3-72
CR3015V.....R.....P.NS	TRN.A.YT.E.A.DKTK	3-20
CR3018V.....R.....P.NS	TRN.A.YT.E.A.DKTK	3-23

VL

	FR1	CDR1	FR2	CDR2	FR3	CDR3	FR4	
	DIELTQSPSSLSASV	GRDVTITC	RASQSISSYLN	WYQQKPGKAPK	LLIYAASLQSGVPSR	FSGSGSDT	PTLTITISLQPED	FATYYC
SVO2A20V2-13
CR3001Q.M.....H.....G..N..AVTTSFR
CR3006D.-AE.VA	L.QT.RQGD	SLR.Y.ASQV.VGKNNRPI.D
CR3015D.-AE.VA	L.QT.RQGD	SLR.Y.ASQV.VGKNNRPI.D

FIG. 2. Deduced protein sequences of VH and VL domains of clones that bind to SARS-CoV. FR, framework region; CDR, complementarity-determining region. Dots indicate sequence identity to the consensus sequence.

To map the epitopes of CR3009 and CR3018 IgG on the N protein, Pepscan analysis was used. The results obtained with IgG CR3018 and overlapping peptides derived from the N protein are shown in Fig. 4D. IgG CR3018 reacted with a continuous series of linear and looped peptides, starting with the sequences GPQSNQRSAPRITFG and PQSNQRSAPRITFGG, respectively, and both ending with the peptide RSAPRITFGGPTDST, thereby having the minimal sequence RSA PRITFG in common. For IgG CR3009 and all other six IgGs, the N protein Pepscan analysis did not reveal significant binding to any of the N protein-derived peptides (data not shown), which is in agreement with the results from Fig. 4A. Furthermore, it suggests that CR3009 recognizes a nonlinear epitope.

Analysis of N binding by EM. Ultrathin-section EM was used to investigate the binding of MABs CR3009 and CR3018 to native N in whole virions in more detail. Localization of dense gold-label within SARS-CoV virions was observed when infected Vero cells were stained with CR3009 or CR3018, whereas a control human IgG1 MAB does not induce any label (Fig. 5). The localization of the gold label clearly indicates that N is retained within the virion.

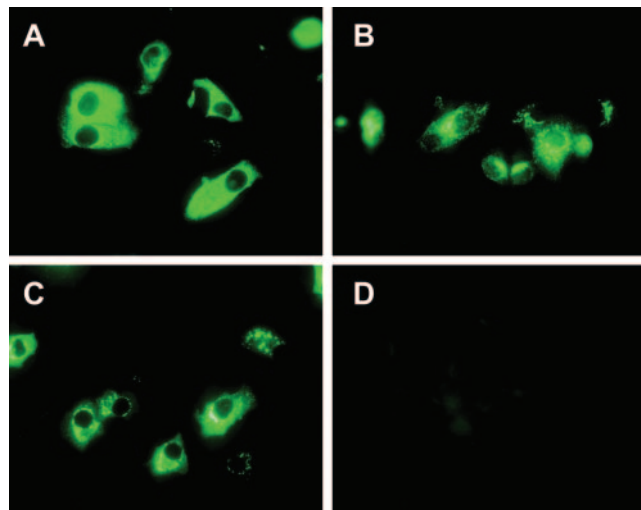


FIG. 3. Binding of the IgGs to SARS-CoV-infected Vero cells. Immunofluorescent staining with IgG CR3009 (A), CR3014 (B), CR3018 (C), or negative control IgG (D) is shown.

Characterization of antibodies binding S protein. The interaction of the IgGs with S protein, the major protein in the viral envelope, was evaluated. Binding of the IgGs to the full-length S protein on 293T cells was first investigated by flow cytometry. This analysis showed that IgGs CR3006, CR3013, CR3014, and CR3015 specifically bound S-protein-transfected cells (Fig. 6A). To further localize the binding site of these IgGs within the S protein, binding to a recombinant soluble fragment encompassing S protein residues 1 to 565 (S565) was tested. Within the S protein binding panel, all IgGs except CR3015 bound to fragment S565 (Fig. 6A). Recently, Wong et al. (42) attributed the binding site of the ACE2 receptor to a region comprising amino acid residues 318 to 510 within the S protein. To further map the binding site of the MABs, binding to a recombinant fragment comprising residues 318 to 510 was evaluated. Figure 6A shows that only CR3006, CR3013, and CR3014 were able to bind the S318-510 fragment. As shown in Fig. 6B, IgG CR3014 appears to bind S565 with a higher affinity than IgGs CR3006 and CR3013. At the scFv/phage level it had already been observed that clones CR3013 and CR3014 compete for binding to the SARS-CoV (data not shown). In addition, sequence analysis revealed that the VH and VL genes of CR3013 and CR3014 are highly homologous, varying in only three residues in the CDR3 of the VH domain (Fig. 2). To confirm these findings and to study the antibody binding sites in more detail, a competition ELISA on immobilized S565 fragment was performed (Fig. 6C). This analysis revealed that MAB CR3006 competed with all MABs. MAB CR3013 efficiently competed with unlabeled CR3013 and CR3014, but to a lesser extent with CR3006 and MAB CR3014 only efficiently competed with unlabeled CR3014. Together, this demonstrates that MABs CR3006, CR3013, and CR3014 recognize the same or overlapping epitope, but with different affinities.

We next evaluated whether MABs CR3006, CR3013, and CR3014 were capable of binding the S protein of other human SARS-CoV isolates. Alignment of residues 318 to 510 of the S protein of 114 human SARS-CoV isolates, which have been published in GenBank, revealed eight different S sequences (Table 1) that were not identical to the same region of the FM1 S protein, which was used in the present study. The eight sequences were expressed as recombinant S318-510 fragments, and the binding of MABs CR3006, CR3013, and CR3014 to

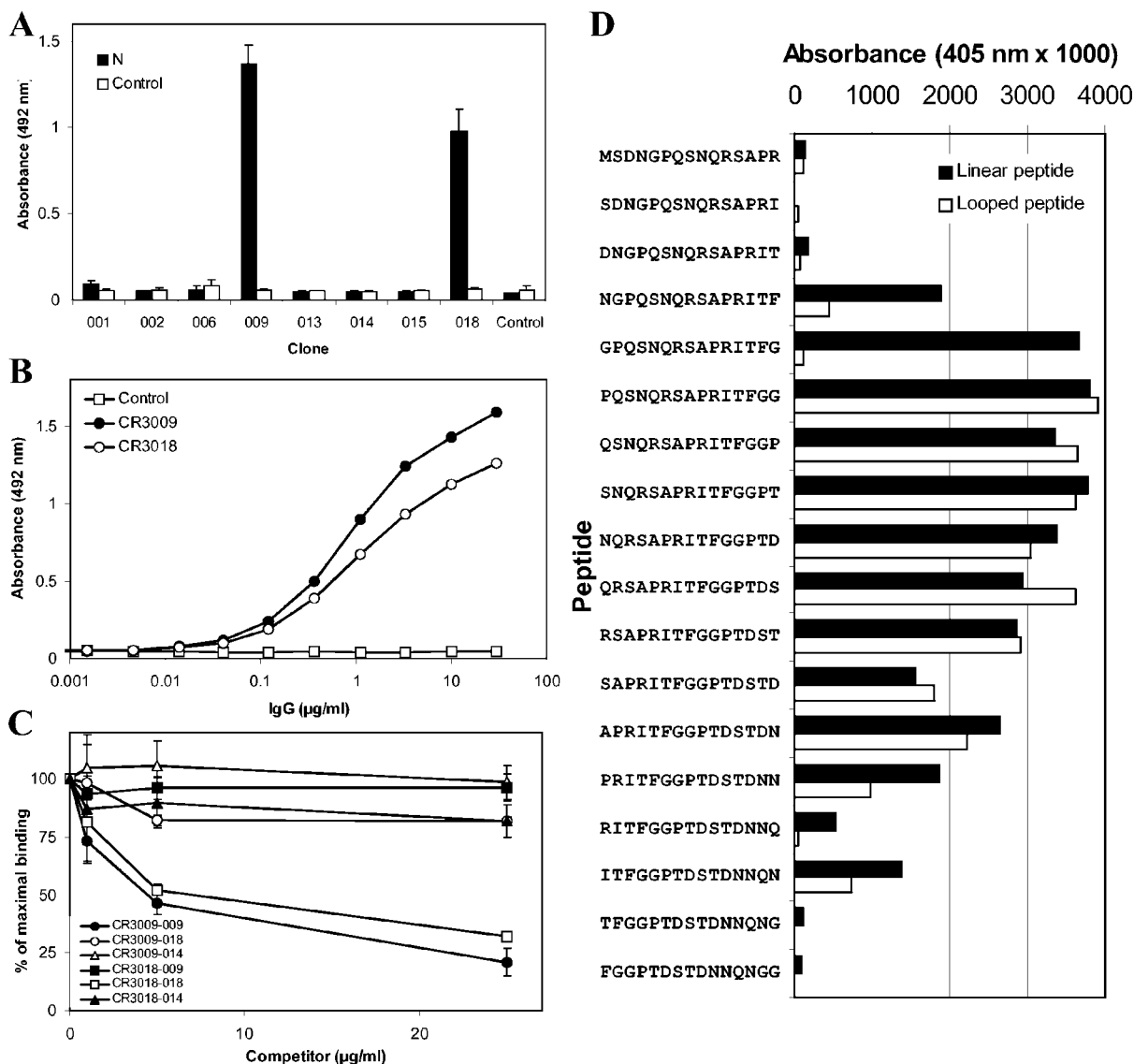


FIG. 4. Binding of human IgGs to N protein analyzed by ELISA. (A) Binding of human IgGs to N protein or an irrelevant negative control protein captured via an anti-myc antibody. (B) Titration of IgGs CR3009, CR3018, and negative control IgG to the N protein. (C) Competition ELISA on immobilized SARS-CoV for binding to N protein. The binding of biotinylated IgG CR3009 was analyzed in the presence of increasing amounts of competitor IgG CR3009, CR3018, or CR3014. The binding of biotinylated IgG CR3018 was analyzed in the presence of competitor IgG CR3009, CR3018, or CR3014. The binding is expressed as the percentage of binding without competitor. (D) Pepscan analysis of N-protein-derived peptides with IgG CR3018. On the y axis, the 18 amino-terminal peptides of N protein are depicted. The binding to linear or looped peptides is indicated as the absorbance at 405 nm ($\times 1,000$) on the x axis.

these variant S318-510 fragments was evaluated. As shown in Fig. 7A, no binding of CR3006 to variants 5 and 7 was observed, which indicates a possible contribution of amino acid residues Y442 and F360, L472, D480, or T487 to the epitope of CR3006. All variant S318-510 fragments were recognized by CR3013 and CR3014. However, binding of CR3013 and CR3014 to variant 6 appears to be reduced compared to the other variants. To further investigate the epitope of CR3014, binding to variant 6 was evaluated quantitatively. When normalized for binding to FM1 S318-510, CR3014 showed significantly reduced reactivity with variant 6 (Fig. 7B), which carries an N479S substitution.

Pepscan analysis with the anti-S IgGs did not identify any

linear S epitopes (data not shown). For IgG CR3001 and CR3002 no significant binding to S or N protein was observed, nor did Pepscan analysis of 2 sets of 2,740 linear and looped peptides covering the complete viral proteome except replicase reveal any recognition sites. This indicates that these IgGs are directed toward conformational epitopes on SARS-CoV-related proteins other than the N and S proteins tested here or replicase.

Inhibition of binding of S565 to Vero cells. To investigate interference of binding of the S1 domain to Vero cells expressing the ACE2 receptor, the natural receptor for SARS-CoV, by IgG CR3014, we performed a flow cytometric inhibition assay. As shown in Fig. 8A, preincubation of fragment S565 in

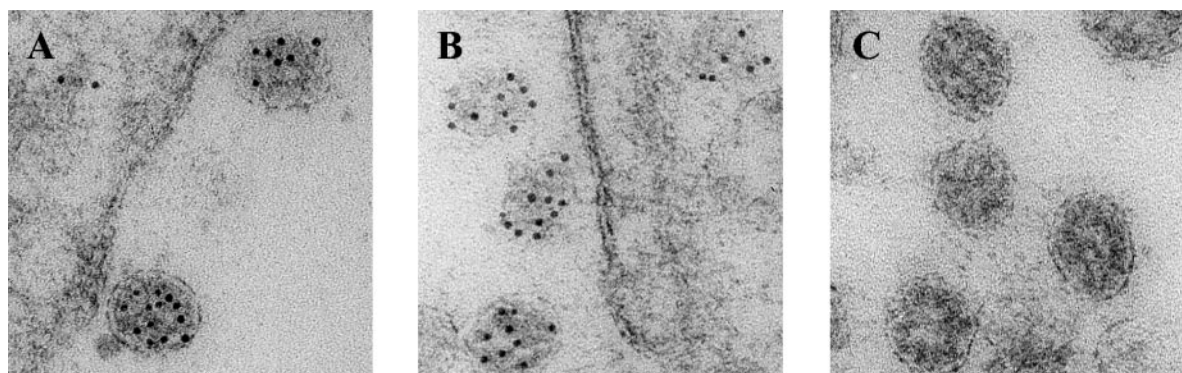


FIG. 5. Visualization of N protein by ultrathin-section immuno-EM. Gold immunolabeling of N protein in SARS-CoV-infected Vero cells with CR3009 (A), CR3018 (B), or negative control MAb (C) was carried out, followed by incubation with 5-nm-colloidal-gold-conjugated secondary antibody.

the presence of 0.5 μ M IgG CR3014 resulted in complete loss of S565 binding to Vero cells, whereas in the presence of anti-N IgG CR3018, S565-receptor binding remained unaffected (Fig. 8B). Interestingly, IgG CR3006 only partially prevented binding of the S565 fragment to Vero cells (Fig. 8C).

In vitro neutralizing activity of antibodies to SARS-CoV. A primary SARS-CoV neutralization assay with Vero cells was performed to determine which MABs possess neutralizing properties. Of the scFv tested, CR3013 and CR3014 readily neutralized SARS-CoV strains FM1 (Fig. 9). Neutralization by CR3013 and CR3014 IgG was investigated in more detail by using various amounts of a different SARS-CoV isolate HKU-39849, obtained from a patient who died of SARS (12, 23). Serial twofold dilutions of CR3013, CR3014, and control IgG starting at 300 nM were incubated in the presence of 10, 30, and 100 TCID₅₀ of SARS-CoV for 1 h at 37°C prior to incubation with Vero cells. Reformatting of scFv to IgG resulted in a two- to fivefold-increased neutralizing potency for CR3013 and CR3014. Complete protection from infectivity of 100 TCID₅₀ was reached at 170 nM for CR3013 and 42 nM for CR3014 (Fig. 9). The lower concentration of CR3014 required to completely prevent infectivity indicates that IgG CR3014 is more potent than CR3013, in accordance with its superior binding capacity. CR3006 did not show neutralizing capacity at the normal IgG dilution range; however, subsequent neutralization assays revealed that CR3006 was capable of neutralizing SARS-CoV but only at high concentrations in the micromolar range (data not shown).

DISCUSSION

We describe here the characterization of eight different fully human IgGs directed to SARS-CoV that were isolated from semisynthetic human antibody libraries. Since complete SARS-CoV virions, rather than a single recombinant protein or fragment thereof, were used as antigen for selections, MABs against different proteins in their natural conformation were isolated. Target identification revealed that two MABs reacted with the N protein, and EM performed with both MABs enabled us to visualize the presence of N protein within virions produced by SARS-CoV-infected Vero cells.

The epitopes of these noncompeting MABs, CR3009 and

CR3018, were investigated in more detail by using Pepscan analysis. Through this approach, the minimal binding site of CR3018 was mapped to residues 11 to 19 of the N protein, which corresponds to the sequence RSAPRITFG. Interestingly, this linear epitope is conserved in the N protein sequence of all published human SARS-CoV and animal SARS-CoV-like isolates but is absent in other members of the family of *Coronaviridae*. Assessment of antigenic peptides derived from SARS-CoV structural proteins revealed that 9 of 31 sera from SARS patients tested reacted with a peptide composed of residues 1 to 23 of N protein (41). This indicates that a significant proportion of the SARS patients develops antibodies to N protein, which are directed to an epitope similar to that recognized by CR3018. Future studies should reveal the level of sequence homology between human MABs isolated from the antibody repertoire of patients with SARS and antibody CR3018, which was isolated from a semisynthetic scFv phage display library. Epitope mapping of MAB CR3009 was unsuccessful, presumably because CR3009 recognizes a nonlinear epitope. Besides a large number of linear epitopes (16, 41), the N protein contains two major conformational epitopes recognized by the sera of SARS patients (5). These characteristics of both CR3009 and CR3018 could be exploited in a diagnostic test specific for SARS-CoV.

At present, solid proof of SARS-CoV infection is provided after isolation of the virus from a clinical specimen, a confirmed positive PCR for SARS-CoV or detection of antibody seroconversion. Virus isolation is time-consuming, and PCR requires technical equipment, which is not available in every local hospital. In the majority of the patients, seroconversion is only detectable from the second or third week after disease onset (24, 26, 31), making this late and retrospective diagnostic tool ineffective for quarantine measures. Furthermore, antibodies to SARS-CoV or related viruses have already been detected in blood samples taken from healthy individuals 2 years before the most recent SARS outbreak (30, 45). Taken together, these findings emphasize the need for an instant and more accurate laboratory test for the early diagnosis of SARS. MABs that specifically detect SARS-CoV proteins may therefore greatly facilitate the development of a SARS-CoV-specific immunoassay.

In addition to N protein MABs, four MABs to the S protein

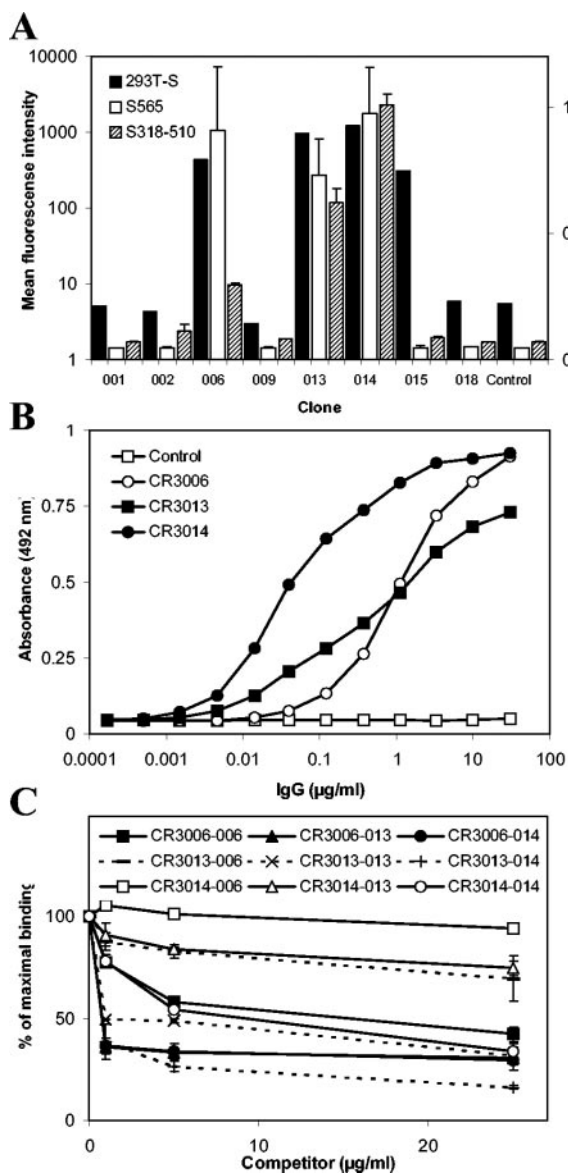


FIG. 6. Analysis of the binding of human IgGs to S protein. (A) Binding of IgGs to S-protein-transfected 293T cells with fluorescence-activated cell sorting indicated as the mean fluorescence intensity or to recombinant S565 or S318-510 fragment as determined by ELISA. (B) Titration of IgGs CR3006, CR3013, CR3014, and negative control IgG (Control) in an S565 fragment-coated ELISA. (C) Competition ELISA on immobilized S565. The binding of biotinylated IgG CR3006 (solid symbols) was analyzed in the presence of increasing amounts of competitor IgG CR3006, CR3013, or CR3014. The binding of biotinylated IgG CR3013 (dotted lines) was analyzed in the presence of competitor IgG CR3006, CR3013, or CR3014, and the binding of biotinylated IgG CR3014 (open symbols) was analyzed in the presence of competitor IgG CR3006, CR3013, or CR3014. Binding is expressed as the percentage of binding without competitor.

were isolated, three of which were capable of effectively neutralizing SARS-CoV infectivity in vitro. The epitope of the nonneutralizing antibody, CR3015, is located outside the region comprising residues 1 to 565 and could be located within the S2 domain. Human antibodies binding to different epitopes in the S2 domain protein have been described previously (41,

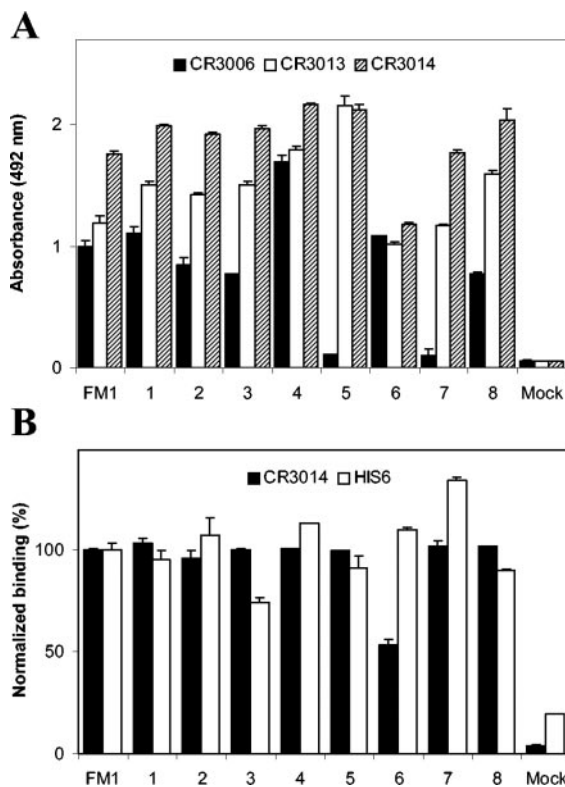


FIG. 7. Binding of human IgGs to recombinant S318-510 fragment with naturally occurring mutations. (A) Binding of CR3006, CR3013, and CR3014 to recombinant S318-510 fragments and variants thereof by ELISA. (B) Binding of CR3014 and anti-HIS6 MAb to recombinant S318-510 fragments, which was normalized for binding to FM1 S318-510.

44). Sui et al. reported previously eight scFv, all directed to the S1 domain (residues 1 to 672), of which only one, 80R, was capable of neutralizing SARS-CoV infectivity (38). This indicates that not all antibodies binding to the S1 domain of the S protein do interfere with the infectivity of SARS-CoV. MAbs CR3006, CR3013, and CR3014 described here compete for binding to the S1 domain with different affinities and neutralize SARS-CoV. However, antibody affinity and neutralizing potency do not necessarily correlate. Traggiai et al. isolated two types of neutralizing MAbs with Epstein-Barr virus transformation. Some MAbs showed neutralizing titers proportional to their degree of binding, whereas others showed low-avidity binding in spite of efficient viral neutralization (40).

We demonstrated that the epitopes of our neutralizing MAbs are located within the previously identified minimal ACE2 receptor-binding region of the S protein; a more precise characterization of the epitope by using Pepscan analysis failed. Most likely, MAb CR3014 recognizes a more complex conformational epitope within the S1 domain that cannot be detected by this technique. This suggests that the MAb CR3014 binding site is different from that of MAb 80R (38), which was shown to remain partially intact under denaturing and reducing conditions. Also, deglycosylation of the S1 domain did not prevent R80 from binding to its epitope. Binding studies with variant recombinant S318-510 fragments revealed that the epitope of CR3014 is conserved in the S proteins of all

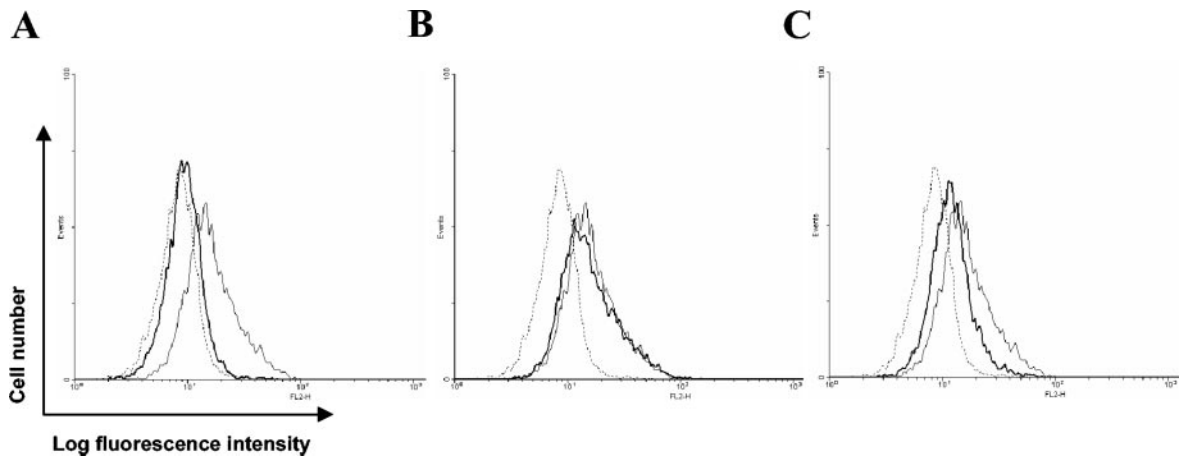


FIG. 8. Inhibition of the interaction of S565 with Vero cells by human IgG measured by fluorescence-activated cell sorting. Vero cells were incubated with S-protein-derived fragment S565 in the absence (thin line) or presence (solid line) of IgG CR3014 (A), CR3018 (B), or CR3006 (C). The dotted line represents the negative control (irrelevant myc-tagged protein).

human SARS-CoV isolates described in Table 1. Reduced reactivity with a variant S318-510 fragment harboring a N479S substitution suggests a substantial contribution of this residue to binding of CR3014. Residue N479 may either be directly involved in binding of CR3014 by being part of the antibody binding site or, alternatively, contribute to a correct conformation of the antibody binding site. The epitope of CR3006 was completely destroyed by the introduction of naturally occurring amino acid substitutions of residues Y442 or F360, L472, D480, and T487, as are present in two different SARS-CoV isolates. One of these isolates was collected in December 2003 from the last infected patient not related to a laboratory-acquired SARS infection (6). These data illustrate the importance of evaluating the specificity of anti-S MAbs for a wide variety of SARS-CoV isolates.

The development of neutralizing antibodies in patients with

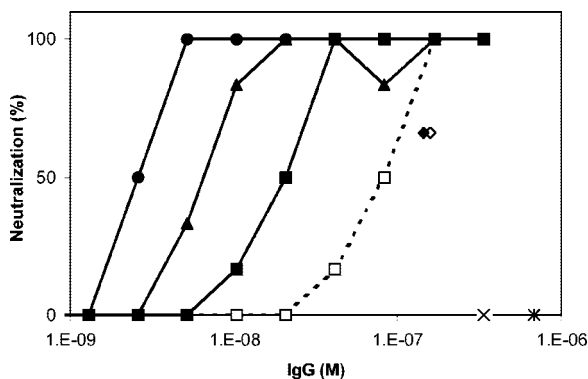


FIG. 9. SARS-CoV neutralizing activity of scFv and IgGs. Neutralization is shown as percentage. Protection against 100 TCID₅₀ SARS-CoV in two of three culture wells by scFv CR3013 (◇) and CR3014 (◆) is indicated. No protection by scFv CR3006 (*) was observed. The neutralization value shown for each IgG is the percentage of culture wells protected from infection with SARS-CoV. The experiments were performed twice in triplicate. Results for neutralization by serially diluted IgG CR3014 of 10 (●), 30 (▲), or 100 (■) TCID₅₀ of SARS-CoV and 100 and 10 TCID₅₀ of SARS-CoV by CR3013 (□) and control IgG (×), respectively, are shown.

SARS is similar to that observed in other acute viral infectious diseases such as hepatitis A (19). The preventive value of IgG against hepatitis A infection was demonstrated as early as 1945 (36), and prevention of rabies after exposure requires the administration of immunoglobulin prepared from hyperimmune sera in combination with vaccine (33). Based on these observations and the successful use of a recombinant MAb against respiratory syncytial virus that prevents disease in high-risk infants (20), immunoprophylaxis of SARS-CoV infection with MAbs might be an option for the control of SARS (18).

To this end, we evaluated whether the neutralizing capacity of CR3014 in vitro can abolish the infectivity of SARS-CoV in ferrets, essentially as described by Emini et al., for infectivity of human immunodeficiency virus type 1 (HIV-1) in chimpanzees (11). In this ferret model, infection of the animals via the intratracheal route leads to massive replication of the virus in the lung and the development of pulmonary SARS-CoV-associated lesions accompanied by various degrees of nonlethal clinical disease (28). High virus titers were observed in the lungs of control ferrets on day 4, which dropped at day 7, thereby following the natural course of infection with SARS-CoV. Animals that received a combination of CR3014 and virus had almost undetectable titers of SARS-CoV in their lungs. In a follow-up study, we demonstrated that prophylactic administration of CR3014 at 10 mg/ml reduced replication of SARS-CoV in the lungs of infected ferrets, prevented SARS-CoV-induced macroscopic lung pathology, and abolished the shedding of virus in pharyngeal secretions (39).

Thus, SARS-CoV neutralizing antibodies may be used to prevent infection in people exposed to the SARS-CoV, such as hospital personnel caring for suspected SARS patients, and may also be applied for the early treatment of infected individuals to avoid the onset of severe SARS disease and to lower the chance of spreading the virus to exposed individuals.

ACKNOWLEDGMENTS

We thank Jerry W. Slootstra and Rob H. Melen for performing the Pepsican analysis, Anette Teichert for supplying high-titer SARS-CoV-producing cells, and Andrea Männel for her expertise and reliable work in immuno-EM.

REFERENCES

- Biel, S. S., and H. R. Gelderblom. 1999. Electron microscopy of viruses, p. 111–147. In A. Cann (ed.), *Virus cell culture: a practical approach*. Oxford University Press, Oxford, England.
- Boel, E., S. Verlaan, M. J. Poppelier, N. A. Westerdaal, J. A. Van Strijp, and T. Logtenberg. 2000. Functional human monoclonal antibodies of all isotypes constructed from phage display library-derived single-chain Fv antibody fragments. *J. Immunol. Methods* **239**:153–166.
- Bonavia, A., B. D. Zelus, D. E. Wentworth, P. J. Talbot, and K. V. Holmes. 2003. Identification of a receptor-binding domain of the spike glycoprotein of human coronavirus HCoV-229E. *J. Virol.* **77**:2530–2538.
- Cavanagh, D., P. J. Davis, J. H. Darbyshire, and R. W. Peters. 1986. Coronavirus IBV: virus retaining spike glycopolyptide S2 but not S1 is unable to induce virus-neutralizing or haemagglutination-inhibiting antibody, or induce chicken tracheal protection. *J. Gen. Virol.* **67**(Pt. 7):1435–1442.
- Chen, Z., D. Pei, L. Jiang, Y. Song, J. Wang, H. Wang, D. Zhou, J. Zhai, Z. Du, B. Li, M. Qiu, Y. Han, Z. Guo, and R. Yang. 2004. Antigenicity analysis of different regions of the severe acute respiratory syndrome coronavirus nucleocapsid protein. *Clin. Chem.* **50**:988–995.
- Chinese SARS Molecular Epidemiology Consortium. 2004. Molecular evolution of the SARS coronavirus during the course of the SARS epidemic in China. *Science* **303**:1666–1669.
- Cinatl, J., B. Morgenstern, G. Bauer, P. Chandra, H. Rabenau, and H. W. Doerr. 2003. Glycyrrhizin, an active component of liquorice roots, and replication of SARS-associated coronavirus. *Lancet* **361**:2045–2046.
- de Kruijf, J., E. Boel, and T. Logtenberg. 1995. Selection and application of human single chain Fv antibody fragments from a semi-synthetic phage antibody display library with designed CDR3 regions. *J. Mol. Biol.* **248**:97–105.
- Donnelly, C. A., A. C. Ghani, G. M. Leung, A. J. Hedley, C. Fraser, S. Riley, L. J. Abu-Raddad, L. M. Ho, T. Q. Thach, P. Chau, K. P. Chan, T. H. Lam, L. Y. Tse, T. Tsang, S. H. Liu, J. H. Kong, E. M. Lau, N. M. Ferguson, and R. M. Anderson. 2003. Epidemiological determinants of spread of causal agent of severe acute respiratory syndrome in Hong Kong. *Lancet* **361**:1761–1766.
- Drosten, C., S. Gunther, W. Preiser, S. van der Werf, H. R. Brodt, S. Becker, H. Rabenau, M. Panning, L. Kolesnikova, R. A. Fouchier, A. Berger, A. M. Burguiere, J. Cinatl, M. Eickmann, N. Escriou, K. Grywna, S. Kramme, J. C. Manuguerra, S. Muller, V. Rickerts, M. Stürmer, S. Vieth, H. D. Klenk, A. D. Osterhaus, H. Schmitz, and H. W. Doerr. 2003. Identification of a novel coronavirus in patients with severe acute respiratory syndrome. *N. Engl. J. Med.* **348**:1967–1976.
- Emini, E. A., P. L. Nara, W. A. Schleif, J. A. Lewis, J. P. Davide, D. R. Lee, J. Kessler, S. Conley, S. Matsushita, S. D. Putney, R. J. Gerety, and J. W. Eichberg. 1990. Antibody-mediated in vitro neutralization of human immunodeficiency virus type 1 abolishes infectivity for chimpanzees. *J. Virol.* **64**:3674–3678.
- Fouchier, R. A., T. Kuiken, M. Schutten, G. van Amerongen, G. J. van Doornum, B. G. van den Hoogen, M. Peiris, W. Lim, K. Stohr, and A. D. Osterhaus. 2003. Aetiology: Koch's postulates fulfilled for SARS virus. *Nature* **423**:240.
- Gallagher, T. M., S. E. Parker, and M. J. Buchmeier. 1990. Neutralization-resistant variants of a neurotropic coronavirus are generated by deletions within the amino-terminal half of the spike glycoprotein. *J. Virol.* **64**:731–741.
- Geysen, H. M., S. J. Barteling, and R. H. Meloen. 1985. Small peptides induce antibodies with a sequence and structural requirement for binding antigen comparable to antibodies raised against the native protein. *Proc. Natl. Acad. Sci. USA* **82**:178–182.
- Geysen, H. M., R. H. Meloen, and S. J. Barteling. 1984. Use of peptide synthesis to probe viral antigens for epitopes to a resolution of a single amino acid. *Proc. Natl. Acad. Sci. USA* **81**:3998–4002.
- Guo, J. P., M. Petric, W. Campbell, and P. L. McGeer. 2004. SARS corona virus peptides recognized by antibodies in the sera of convalescent cases. *Virology* **324**:251–256.
- Havenga, M. J., A. A. Lemckert, J. M. Grimbergen, R. Vogels, L. G. Huisman, D. Valerio, A. Bout, and P. H. Quax. 2001. Improved adenovirus vectors for infection of cardiovascular tissues. *J. Virol.* **75**:3335–3342.
- Holmes, K. V. 2003. SARS coronavirus: a new challenge for prevention and therapy. *J. Clin. Investig.* **111**:1605–1609.
- Kawai, H., and S. M. Feinstone. 2000. Acute viral hepatitis, p. 1279–1297. In B. J. Mandell and R. Dolin (ed.), *Principles and practice of infectious diseases*, 5th ed., vol. 1. Churchill Livingstone, Philadelphia, Pa.
- Keller, M. A., and E. R. Stiehm. 2000. Passive immunity in prevention and treatment of infectious diseases. *Clin. Microbiol. Rev.* **13**:602–614.
- Ksiazek, T. G., D. Erdman, C. S. Goldsmith, S. R. Zaki, T. Peret, S. Emery, S. Tong, C. Urbani, J. A. Comer, W. Lim, P. E. Rollin, S. F. Dowell, A. E. Ling, C. D. Humphrey, W. J. Shieh, J. Guarnier, C. D. Paddock, P. Rota, B. Fields, J. DeRisi, J. Y. Yang, N. Cox, J. M. Hughes, J. W. LeDuc, W. J. Bellini, and L. J. Anderson. 2003. A novel coronavirus associated with severe acute respiratory syndrome. *N. Engl. J. Med.* **348**:1953–1966.
- Kubo, H., Y. K. Yamada, and F. Taguchi. 1994. Localization of neutralizing epitopes and the receptor-binding site within the amino-terminal 330 amino acids of the murine coronavirus spike protein. *J. Virol.* **68**:5403–5410.
- Kuiken, T., R. A. Fouchier, M. Schutten, G. F. Rimmelzwaan, G. van Amerongen, D. van Riel, J. D. Laman, T. de Jong, G. van Doornum, W. Lim, A. E. Ling, P. K. Chan, J. S. Tam, M. C. Zambon, R. Gopal, C. Drosten, S. van der Werf, N. Escriou, J. C. Manuguerra, K. Stohr, J. S. Peiris, and A. D. Osterhaus. 2003. Newly discovered coronavirus as the primary cause of severe acute respiratory syndrome. *Lancet* **362**:263–270.
- Li, G., X. Chen, and A. Xu. 2003. Profile of specific antibodies to the SARS-associated coronavirus. *N. Engl. J. Med.* **349**:508–509.
- Li, W., M. J. Moore, N. Vasilieva, J. Sui, S. K. Wong, M. A. Berne, M. Somasundaran, J. L. Sullivan, K. Luzuriaga, T. C. Greenough, H. Choe, and M. Farzan. 2003. Angiotensin-converting enzyme 2 is a functional receptor for the SARS coronavirus. *Nature* **426**:450–454.
- Liu, X., Y. Shi, P. Li, L. Li, Y. Yi, Q. Ma, and C. Cao. 2004. Profile of antibodies to the nucleocapsid protein of the severe acute respiratory syndrome (SARS)-associated coronavirus in probable SARS patients. *Clin. Diagn. Lab. Immunol.* **11**:227–228.
- Marks, J. D., H. R. Hoogenboom, T. P. Bonnert, J. McCafferty, A. D. Griffiths, and G. Winter. 1991. By-passing immunization. Human antibodies from V-gene libraries displayed on phage. *J. Mol. Biol.* **222**:581–597.
- Martina, B. E., B. L. Haagmans, T. Kuiken, R. A. Fouchier, G. F. Rimmelzwaan, G. Van Amerongen, J. S. Peiris, W. Lim, and A. D. Osterhaus. 2003. Virology: SARS virus infection of cats and ferrets. *Nature* **425**:915.
- Nicholls, J. M., L. L. Poon, K. C. Lee, W. F. Ng, S. T. Lai, C. Y. Leung, C. M. Chu, P. K. Hui, K. L. Mak, W. Lim, K. W. Yan, K. H. Chan, N. C. Tsang, Y. Guan, K. Y. Yuen, and J. S. Peiris. 2003. Lung pathology of fatal severe acute respiratory syndrome. *Lancet* **361**:1773–1778.
- Pearson, H. 2004. Antibodies to SARS-like virus hint at repeated infections. *Nature* **427**:185.
- Peiris, J. S., C. M. Chu, V. C. Cheng, K. S. Chan, I. F. Hung, L. L. Poon, K. I. Law, B. S. Tang, T. Y. Hon, C. S. Chan, K. H. Chan, J. S. Ng, B. J. Zheng, W. L. Ng, R. W. Lai, Y. Guan, and K. Y. Yuen. 2003. Clinical progression and viral load in a community outbreak of coronavirus-associated SARS pneumonia: a prospective study. *Lancet* **361**:1767–1772.
- Peiris, J. S., S. T. Lai, L. L. Poon, Y. Guan, L. Y. Yam, W. Lim, J. Nicholls, W. K. Yee, W. W. Yan, M. T. Cheung, V. C. Cheng, K. H. Chan, D. N. Tsang, R. W. Yung, T. K. Ng, and K. Y. Yuen. 2003. Coronavirus as a possible cause of severe acute respiratory syndrome. *Lancet* **361**:1319–1325.
- Rupprecht, C. E., C. A. Hanlon, and T. Hemachudha. 2002. Rabies re-examined. *Lancet Infect. Dis.* **2**:327–343.
- Slootstra, J. W., W. C. Puijk, G. J. Ligtoet, J. P. Langeveld, and R. H. Meloen. 1996. Structural aspects of antibody-antigen interaction revealed through small random peptide libraries. *Mol. Divers.* **1**:87–96.
- Snijder, E. J., P. J. Bredenbeek, J. C. Dobbe, V. Thiel, J. Ziebuhr, L. L. Poon, Y. Guan, M. Rozanov, W. J. Spaan, and A. E. Gorbalenya. 2003. Unique and conserved features of genome and proteome of SARS-coronavirus, an early split-off from the coronavirus group 2 lineage. *J. Mol. Biol.* **331**:991–1004.
- Stokes, J., and J. R. Neefe. 1945. The prevention and attenuation of infectious hepatitis by gamma globulin. *JAMA* **127**:144–145.
- Subbarao, K., J. McAuliffe, L. Vogel, G. Fahle, S. Fischer, K. Tatti, M. Packard, W. J. Shieh, S. Zaki, and B. Murphy. 2004. Prior infection and passive transfer of neutralizing antibody prevent replication of severe acute respiratory syndrome coronavirus in the respiratory tract of mice. *J. Virol.* **78**:3572–3577.
- Sui, J., W. Li, A. Murakami, A. Tamin, L. J. Matthews, S. K. Wong, M. J. Moore, A. S. Tallarico, M. Olurinde, H. Choe, L. J. Anderson, W. J. Bellini, M. Farzan, and W. A. Marasco. 2004. Potent neutralization of severe acute respiratory syndrome (SARS) coronavirus by a human mAb to S1 protein that blocks receptor association. *Proc. Natl. Acad. Sci. USA* **101**:2536–2541.
- ter Meulen, J., A. B. Bakker, E. N. van den Brink, G. J. Weverling, B. E. Martina, B. L. Haagmans, T. Kuiken, J. de Kruijf, W. Preiser, W. Spaan, H. R. Gelderblom, J. Goudsmit, and A. D. Osterhaus. 2004. Human monoclonal antibody as prophylaxis for SARS coronavirus infection in ferrets. *Lancet* **363**:2139–2141.
- Traggiai, E., S. Becker, K. Subbarao, L. Kolesnikova, Y. Uematsu, M. R. Gismondo, B. R. Murphy, R. Rappuoli, and A. Lanzavecchia. 2004. An efficient method to make human monoclonal antibodies from memory B cells: potent neutralization of SARS coronavirus. *Nat. Med.* **10**:871–875.
- Wang, J., J. Wen, J. Li, J. Yin, Q. Zhu, H. Wang, Y. Yang, E. Qin, B. You, W. Li, X. Li, S. Huang, R. Yang, X. Zhang, L. Yang, T. Zhang, Y. Yin, X. Cui, X. Tang, L. Wang, B. He, L. Ma, T. Lei, C. Zeng, J. Fang, J. Yu, H. Yang, M. B. West, A. Bhatnagar, Y. Lu, N. Xu, and S. Liu. 2003. Assessment of immunoreactive synthetic peptides from the structural proteins of severe acute respiratory syndrome coronavirus. *Clin. Chem.* **49**:1989–1996.
- Wong, S. K., W. Li, M. J. Moore, H. Choe, and M. Farzan. 2004. A 193-amino-acid fragment of the SARS coronavirus S protein efficiently binds angiotensin-converting enzyme 2. *J. Biol. Chem.* **279**:3197–3201.
- Xiao, X., S. Chakraborti, A. S. Dimitrov, K. Gramatikoff, and D. S. Dimitrov. 2003. The SARS-CoV S glycoprotein: expression and functional characterization. *Biochem. Biophys. Res. Commun.* **312**:1159–1164.

44. **Zhang, H., G. Wang, J. Li, Y. Nie, X. Shi, G. Lian, W. Wang, X. Yin, Y. Zhao, X. Qu, M. Ding, and H. Deng.** 2004. Identification of an antigenic determinant on the s2 domain of the severe acute respiratory syndrome coronavirus spike glycoprotein capable of inducing neutralizing antibodies. *J. Virol.* **78**: 6938–6945.
45. **Zheng, B. J., Y. Guan, K. H. Wong, J. Zhou, K. L. Wong, B. W. Y. Young, L. W. Lu, and S. S. Lee.** 2004. SARS-related virus predating SARS outbreak, Hong Kong. *Emerg. Infect. Dis.* **10**:176–178.
46. **Zhou, T., H. Wang, D. Luo, T. Rowe, Z. Wang, R. J. Hogan, S. Qiu, R. J. Bunzel, G. Huang, V. Mishra, T. G. Voss, R. Kimberly, and M. Luo.** 2004. An exposed domain in the severe acute respiratory syndrome coronavirus spike protein induces neutralizing antibodies. *J. Virol.* **78**:7217–7226.